Multi-frequency Observation of Soil Moisture and Vegetation Optical Depth from Space

Tianjie Zhao[1*], Zhiqing Peng[1], Lu Hu[2], and Jiancheng Shi[3]

[1]Aerospace Information Research Institute, Chinese Academy of Sciences, China

[2]International Institute for Earth System Science, Nanjing University, China

[3]National Space Science Center, Chinese Academy of Sciences, China

*zhaotj@aircas.ac.cn

ABSTRACT

Numerous soil moisture (SM) products have been developed for satellite-based microwave remote sensing systems operating at various frequencies. However, it is challenging to make a fair comparison of their sensing capabilities and depth of different frequencies/sensors due to the use of different retrieval algorithms in existing soil moisture products. This study compares two new enhanced-resolution soil moisture datasets from the L-band Soil Moisture Active Passive (SMAP) and the Advanced Microwave Scanning Radiometer 2 (AMSR2) by utilizing the same multi-channel collaborative algorithm (MCCA), termed MCCA SMAP and MCCA AMSR2. The assessment involves a comparison of the satellite soil moisture with 40 globally distributed soil moisture observation networks at regional (dense network) or grid scales. The findings first indicate that both MCCA SMAP and AMSR2 soil moisture products demonstrate superior performance at the regional scale compared to the grid scale. Secondly, for the first time, we have provided evidence that SMAP outperforms AMSR2, with both sensing capabilities decreasing as vegetation cover increases. Furthermore, the analysis of global soil moisture dry-down patterns reveals that SMAP exhibits a lower soil moisture loss rate, an extended soil moisture retention duration, and an effective higher wilting point than AMSR2, which suggests that the L-band contribution depth surpasses that of C-, X-, and Ku-bands at the satellite scale.

Keywords: MCCA, SMAP, AMSR2, soil moisture, dry down

1. Introduction

Surface soil moisture and vegetation optical depth (VOD) are essential variables in the terrestrial ecosystem. The microwave remote sensing has been providing a unique way to obtain the global soil moisture and VOD from space with various spaceborne sensors, including the Advanced Microwave Scanning Radiometer for EOS (AMSR-E), Soil Moisture and Ocean Salinity (SMOS), AMSR2, and Soil Moisture Active Passive (SMAP) etc. Those microwave sensors operating at different frequencies possess differentiated vegetation penetration capabilities and might provide significant information of the Soil-Plant-Atmosphere-Continuum (SPAC) system.

Theoretically, low-frequency microwave retrievals, particularly in the L-band, are expected to exhibit superior performance in soil moisture estimation compared to higher-frequency bands like the C-band and above. This is due to the greater sensitivity of low-frequency signals to the dielectric properties of water and their enhanced ability to penetrate vegetation and soil layers [1]. Several studies have validated this theoretical advantage by comparing satellite-based soil moisture retrievals with in situ observations [2]. However, not all empirical studies have consistently demonstrated that L-band retrievals outperform higher-frequency retrievals. For instance, in the Murrumbidgee River catchment in Australia, AMSR2 soil moisture products were found to outperform SMOS in terms of both absolute and temporal accuracy [3]. These discrepancies highlight the need for a deeper investigation that accounts for variations in algorithmic approaches, rather than solely focusing on frequency differences.

The multi-channel collaborative algorithm (MCCA, [4]) has been effectively applied to diverse sensor configurations, including multi-frequency dual-polarization and single-frequency dual-polarization setups. It has shown success in generating soil moisture products from SMAP [5] and AMSR-E/2 [6] observations. However, comprehensive assessments of the MCCA's performance when applied to SMAP and AMSR-E/2 data are still lacking. By enabling cross-sensor retrievals, MCCA offers a more equitable comparison of soil moisture data across different sensors and frequencies. This makes it an ideal tool for investigating the scientific question of whether SMAP outperforms AMSR2 in soil moisture retrieval, particularly given that both sensors operate at fixed viewing angles but different microwave bands.

To address this question, the study focuses on two key aspects: retrieval accuracy and sensing depth. First, the global performance of soil moisture products from SMAP and AMSR2 is assessed by comparing satellite retrievals with ground-based measurements, laying the groundwork for frequency-based performance evaluations. Second, the study explores global dry-down patterns using MCCA, aiming to compare the sensing depths of SMAP and AMSR2 with respect to the rate of soil moisture loss.

2. Methodology

In this study, we applied the Multi-Channel Collaborative Algorithm (MCCA) [4] to the AMSR-E/2 and SMAP observations for a physically consistent SOIL MOISTURE and VOD

products. The main idea of MCCA is applying the relationship between soil and vegetation property at the core channel to the collaborative channels, with three features: (1) unlike other retrieval algorithms using proxy or iterative procedure to retrieve VOD, an analytical solution was proposed to derive vegetation transmittivity, and then VOD; (2) a general function was proposed to describe relationships of VODs between different channels (frequency, polarization and incidence angle); and (3) brightness temperatures (Tb) at the collaborative channels are derived by the Tb at core channel based on the two-component version of τ-ω model [6], without any assumptions.

In the context of land surface water balance, precipitation leads to an increase in soil moisture, while processes such as infiltration, runoff, and evapotranspiration contribute to its loss. Soil moisture typically decreases through three distinct stages following precipitation. Initially, infiltration predominates when soil moisture exceeds the field capacity. As soil moisture declines below this threshold, evapotranspiration becomes the dominant factor governing moisture loss. This second phase is further subdivided into two stages, influenced by meteorological conditions and soil moisture stress.

The temporal dynamics of soil moisture following precipitation events reveal the soil moisture dry-down curve, which can be described using a loss function, as proposed by McColl et al. [7]. This function characterizes the drying pattern of the soil, with the drying rate serving as a measure of how rapidly soil moisture declines. A key objective of this study is to assess the observation depth of SMAP and AMSR2 through the dry-down rate calculation method outlined by Shellito et al. [8]:

$$\frac{dSM}{dt} = \frac{SM_{n+1} - SM_n}{t_{n+1} - t_n} \quad (1)$$

where t denotes the time since the onset of dry-down (in days), SM denotes the corresponding soil moisture at t, n and n+1 represent consecutive observations. To ensure the robustness of the calculations and prevent the influence of infrequent observations, only data with $t_{n+1} - t_n$ less than 3.5 days are considered in the calculation of drying rate [8]. Given the susceptibility of ascending orbit (PM) data to solar radiation effects, influencing surface thermodynamic balance, this study exclusively employs descending (AM) data to compute the drying rate. This choice aims to minimize discrepancies arising from the differing overpass times of SMAP and AMSR2 observations.

In the process of identifying the dry-down period for this study, soil moisture increments less than 5% of the retrieval range at the grid were disregarded to avoid being truncated by small soil moisture increases [7]. For a qualitative assessment of SMAP and AMSR2 penetration depths, certain constraints were established in computing the drying rate. Firstly, acknowledging that passive microwave emission depth diminishes with rising soil moisture, ensuring a minimal initial emission depth difference between SMAP and AMSR2 was crucial. Thus, in the dry-down detection process, instances where the soil moisture increment before dry-down was less than 3 times the target ubRMSD for SMAP observations (0.12 m^3/m^3) were excluded from the analysis. Secondly, considering the existence of various distinct canonical dry-down patterns, and the influence of surface wind temperature and humidity pressure on the evapotranspiration process, this study focused solely on the drainage stage of the dry-down period. Specifically, analysis was restricted to the period when the SM_n was

greater than the field capacity, and SM_{n+1} fell below field capacity, aiming to mitigate the dominant effect of the evapotranspiration process on the drying rate assessment.

To further evaluate the timescale and magnitude of drying, an exponential model was fitted to each dry-down event containing a minimum of four observations [8], using the following expression:

$$SM(t) = A \times e^{-\frac{t}{\tau}} + SM_f \quad (2)$$

where $SM(t)$ is the observed soil moisture t days after the onset of dry-down, and A, τ, and SM_f are fitted parameters that indicate the magnitude of the soil moisture drying, the estimated dry-down e-folding time scale (in days), and a final low limit of soil moisture, respectively. For each dry-down, these parameters (A, τ, and SM_f) were determined to minimize the sum of squared errors between modeled and retrieved soil moisture values, employing the trust region reflective method. SM_f is constrained between the lowest soil moisture during the dry-down and the lowest soil moisture over the whole period [8]. Unlike the previous section that required data specific to events for drying rate calculation, the entirety of the dry-down period with pre-increment greater than 0.08 (m^3/m^3) was considered in the calculation. The median value of each grid was derived as the outcome for subsequent analysis.

3. Results and discussion

3.1. Comparison of soil moisture retrievals

The dense networks of soil moisture observations, typically situated within specific watersheds, were utilized to represent soil moisture changes at the watershed scale. Comparing satellite retrieval results with these networks enables the evaluation of soil moisture performance at the watershed scale. Fig.1. suggests that the MCCA SMAP and AMSR2 soil moisture products perform well at the regional scale. In terms of temporal variation (R) of soil moisture, SMAP outperformed AMSR2 in 20 out of 23 dense observation networks (Fig. 1a), with respective median R values of 0.787 and 0.664. Most observation networks exhibited R values greater than 0.5. The ubRMSD evaluation results also indicate that SMAP performs better overall (Fig. 1b). For instance, SMAP performs better on ubRMSD than AMSR2 in 17 dense networks, with a median ubRMSD of 0.043 m^3/m^3 for SMAP compared to 0.049 m^3/m^3 for ASMR2.

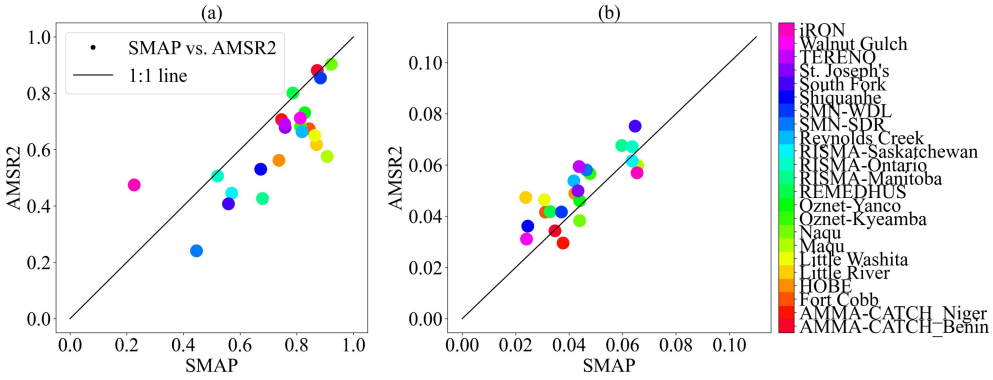

Fig. 1. The dense networks-based validation statistics of SMAP and AMSR2, (a) R, and (b) ubRMSD.

The satellites-based retrieved soil moisture also compared with in situ soil moisture observations from networks at the grid scale. Fig.2. presents the statistical metrics of all grids against vegetation optical depth (VOD) on the horizontal axis. It demonstrates a consistent decline in retrieval performance for both SMAP and AMSR with increasing VOD, as seen in the fitted lines correlating VOD with statistical metrics. The fitting line for SMAP is positioned above that of AMSR2, suggesting that SMAP more accurately captures the dynamics of soil moisture, which is consistent with the result of dense networks. However, both fitting lines have negative slopes, indicating that the received soil emission signals from both SMAP and AMSR2 decreased with increasing vegetation, which makes it more difficult to capture the dynamics of soil moisture. The bias of both is approximately 0 and the fitted lines are very similar in areas with bare soil or sparse vegetation. However, as vegetation increases, the soil moisture of AMSR2 gradually decreases while SMAP remains more stable. This indicates that low-frequency general retrieves wetter soil moisture. Regarding RMSD and ubRMSD, SMAP consistently maintains a lower position relative to AMSR2, indicating lower uncertainty, albeit with both metrics gradually increasing as VOD rises.

Despite AMSR2's utilization of multi-frequency dual-polarization of bright temperatures and possessing more channels than SMAP, its soil moisture retrieval performance is not as good as that of SMAP with only L-band dual-polarization. This highlights the advantage of the L-band in soil moisture retrieval. Additionally, Fig.2 illuminates that most soil moisture in situ stations are currently situated in regions with moderate vegetation coverage (medium VOD). However, the scarcity of in situ stations in areas with bare soil and dense vegetation (high VOD) indicates a need for further deployment in these zones.

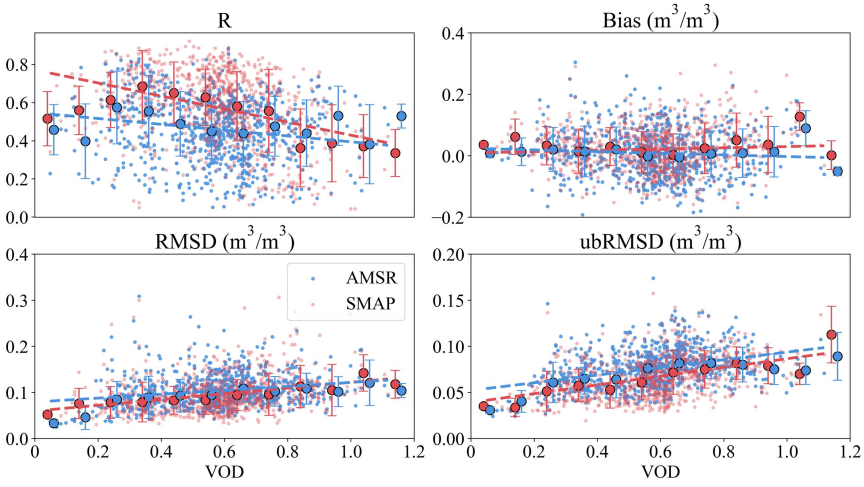

Fig. 2. The relationship of VOD and statistics. The red color represents SMAP, and the blue color represents ASMR2. The dashed lines are the fitting lines of the statistics with changes in VOD, the solid circles with black edges represent the median of the statistics within an interval, and the whistlers represent their standard deviations.

3.2. Comparison of drying rates of soil moisture

Fig. 3 shows the distribution of median drying rates globally for each grid. The stripes in the drying rate of SMAP are caused by its longer sampling frequency. Specifically, only the descending data from SMAP was used, with a nominal sample frequency of 1/3 day-1, and the soil moisture from SMAP has not been under-sampled in this study using the thinning technique in McColl, et al. [7]. The global distribution depicts higher drying rates for both SMAP and AMSR2 in Northern forests, the Amazon, and Malaysian rainforests compared to other regions. Notably, the drying rate (negative value) of soil moisture from SMAP significantly surpasses that of AMSR2, indicating that the loss rate (positive value) of soil moisture based on the SMAP is smaller than that observed by AMSR2. Unlike the readily available data for validation from networks that provide estimates of the surface layer (~5cm), the depth of sensor observations does not always remain the same. Microwave emission depth gradually decreases with increasing soil moisture; thus, the calculation of drying rates is predicated on certain criteria. Specifically, the positive increment of soil moisture preceding the dry-down exceeded 0.12 m^3/m^3, while ensuring that the initial soil moisture observation surpassed the field capacity. This approach aimed to ensure that the initial observational depths of SMAP and AMSR2 were closely aligned. However, subsequent drainage events result in variations in soil moisture, leading to disparities in observational depths between the sensors. When a satellite observes at a deeper depth, the retrieved soil moisture tends to be higher, resulting in a lower loss rate. Consequently, the lower soil loss rate of SMAP can be inferred to be primarily attributed to its deeper observational depth. This finding is consistent with the theory that the longer wavelength of the L-band facilitates observing the response from a deeper depth of the soil surface layer.

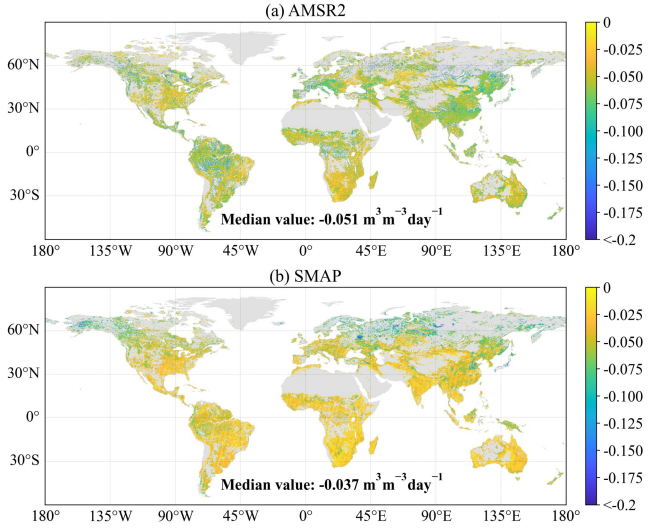

Fig. 3. The global drying rate (unit: m^3 m^{-3} day^{-1}) of AMSR2 and SMAP from April 1, 2015, to March 31, 2017. Gray areas represent filtered soil moisture from AMSR2 or SMAP did not have enough data to calculate drying rates.

3.3. Comparison of drying events of soi moisture

The exponential model was used to fit the dry-down of soil moisture from both AMSR2 and SMAP, excluding results with a determination coefficient lower than 0.7 and confidence intervals of τ approaching 0. Fig. 4 shows the global distribution of median exponential fitting parameters for each grid.

Parameter A represents the magnitude of the dry-down process, indicating minimal differences between SMAP and AMSR2. Notable differences appear in the Amazon Basin, Congo rainforests, and Australian regions, where SMAP's A significantly exceeded AMSR2's. The fitted parameter τ represents the soil moisture memory observed by the satellite. This parameter is closely related to soil depth, as deeper soil layers generally retain soil moisture for longer periods. The global distribution of τ shows spatial heterogeneity. For instance, τ is larger in the eastern than in the western part of the United States. τ is much smaller in boreal forests versus tropical rainforests. This discrepancy is more pronounced in SMAP than in AMSR2. However, median τ values for SMAP and AMSR2 are 4.33 and 4.09 days, respectively, with modes at 3.38 and 2.70 days. The MCCA SMAP median τ agrees closely with Shellito, et al. [8] results (4.08 days), derived from official SCA-V based SMAP data analyzed at in situ stations (also median), while the mode aligns more with McColl, et al. [7] findings (also mode, 3 days). The larger τ in SMAP compared to AMSR2 indicates stronger soil moisture memory in SMAP than in AMSR2, indicative of its deeper observational depth compared to AMSR2.

The parameter SM_f represents the remotely sensed effective wilting point, delineating the threshold below which water availability for plants becomes restricted. As deeper soil layers inherently possess higher water storage capacities than shallower ones, the prevailing trend indicates that a majority of the SM_f values derived from SMAP surpass those obtained from AMSR2. It strongly suggests that the soil moisture retrieved by the L-band likely originates from deeper soil layers in comparison to the observational depth of higher frequencies.

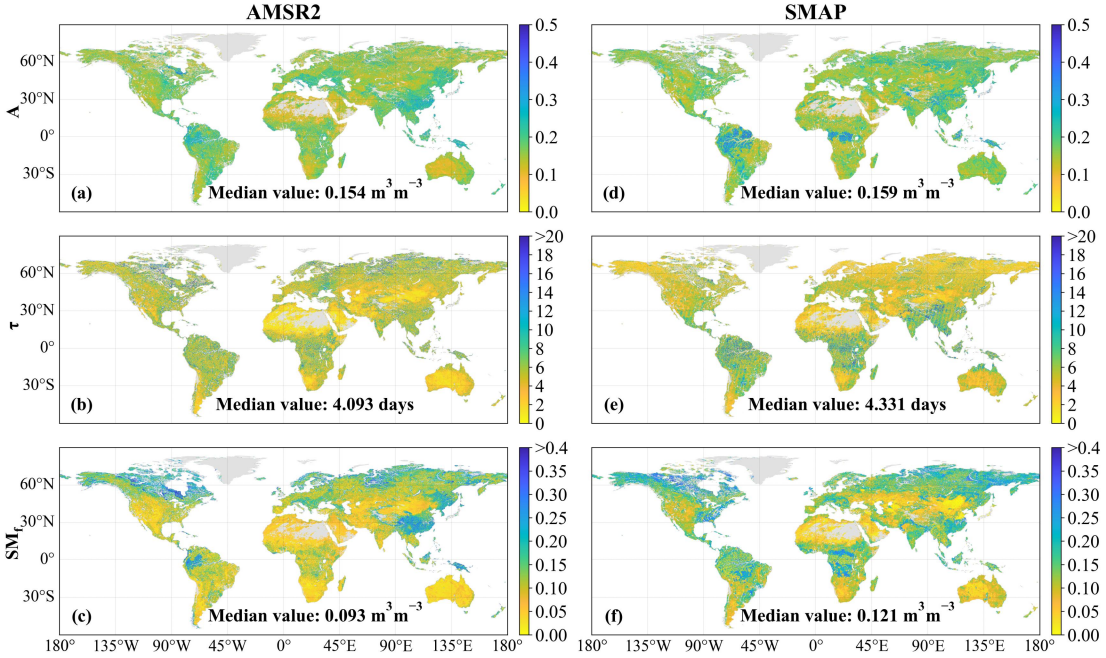

Fig. 4. The exponential model fitted parameters of A, τ, and SM_f for (a-c) AMSR2 and (d-f) SMAP, respectively. Gray areas represent filtered soil moisture from AMSR2 or SMAP did not have enough data to fit the exponential model.

3.4. Comparison of other soi moisture and VOD products

The SMAP MCCA retrievals are inter-compared with other SSM and VOD products (MT-DCA version 5, and DCA, SCA-H, SCA-V from SMAP Level-3 products version 8, and SMAP-IB), showing an analogous spatial pattern. The MCCA derived SSM had the lowest unbiased root mean square error ubRMSE of 0.055 m^3/m^3 followed by SMAP-IB and DCA (0.061 m^3/m^3), and an overall Pearson's correlation coefficient of 0.744 (SMAP-IB performed best with R=0.764) when evaluated against in situ observations from the International Soil Moisture Network (ISMN). Comparable accuracy also found in widely used validation spare network SCAN. The MCCA generates VOD at both vertical and horizontal polarization. While the magnitude of the polarized VODs is lower than other products. MCCA polarized VODs were found to have a good linearity with live biomass and canopy height, though partial saturation exists in the relationship with live biomass of tropical forests but not canopy height. The polarization difference of L-band VODs is mainly located at densely vegetated and arid areas.

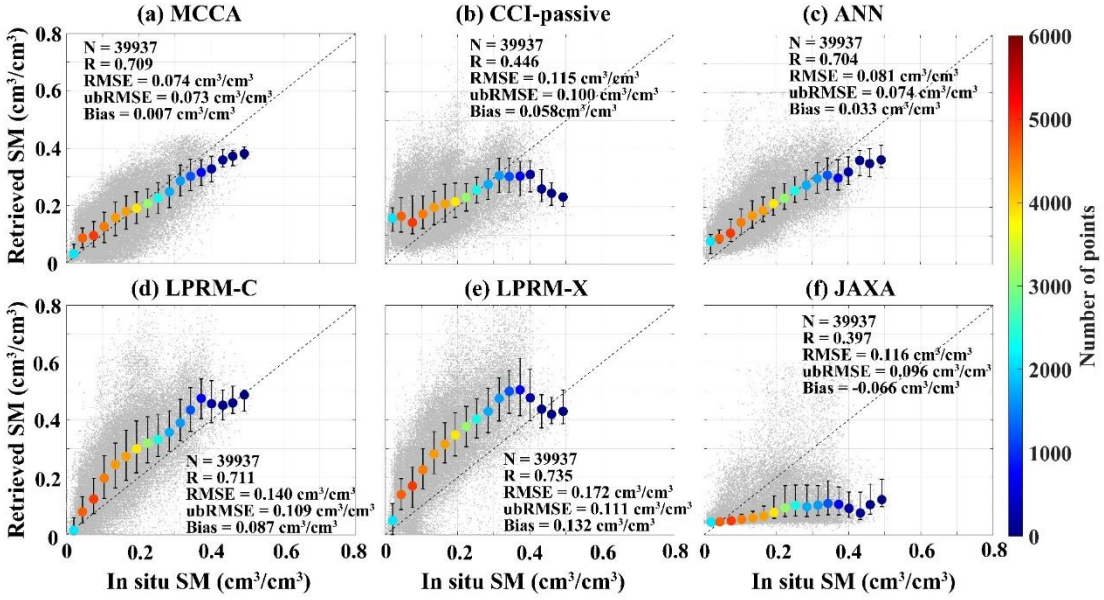

Fig. 5. Total soil moisture scatter with in situ observations. (a) MCCA (b) CCI-passive (c) ANN (d) LPRM-C (e) LPRM-X (f) JAXA. Circles and bars represent the median and inter-quartile ranges of SSM for 0.03 m^3/m^3 wide bins.

The AMSR-E/2 MCCA retrievals are inter-compared with other SSM products (AMSR-ANN, CCI-passive v07.1, LPRM-C/X, JAXA) at ISMN soil moisture networks. Although the R-value of MCCA (0.709) was slightly lower than that of LPRM-X (0.735), MCCA achieved the best scores in terms of RMSE=0.074 m^3/m^3, ubRMSE=0.073 m^3/m^3 and bias=0.007 m^3/m^3 as shown in Fig.5. For the indirect evaluation of VOD with aboveground biomass (AGB) and MODIS NDVI, the MCCA product showed the performance comparable to other products (LPRM-C/X, VODCA-C/X/Ku). MCCA-derived VODs exhibited smooth non-

linear density distribution with AGB and high temporal correlations with MODIS NDVI over most regions, especially for the H-polarized VOD. MCCA-derived VODs can physically present reasonable variations across the microwave spectrum (values of VOD increase with microwave frequency as shown in Fig.6), which is superior to the LPRM and VODCA.

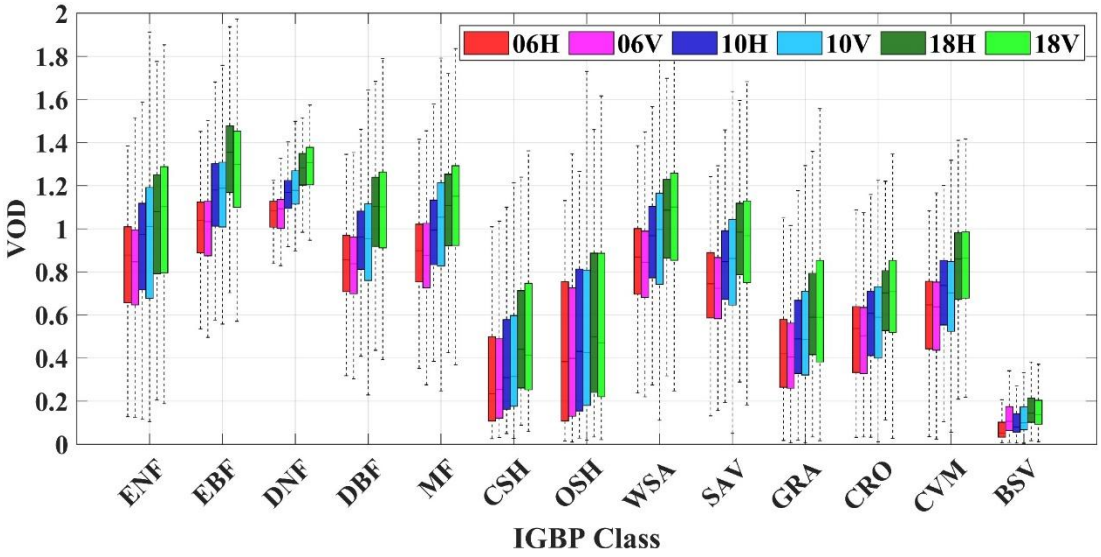

Fig. 6. Boxplot of time-averaged MCCA VODs for different IGBP classes and channels. The central mark within each box shows the median value, and the bottom and top edges mark the extent of the 25th and 75th percentiles. Whiskers include 99.3% of all data.

4. CONCLUSION

Overall, MCCA products developed in this study showed good performance on both SSM and VOD. It is crucial for studies that consider the effects of paired SSM and VOD simultaneously, such as water fluxes in the SPAC system. In addition, the retrieval is implemented on snapshot observations, and MCCA can provide continuous daily data once the daily Tb is updated. It is expected that the MCCA algorithm can be extended to the observations of the upcoming Copernicus Imaging Microwave Radiometer (CMIR) mission.

References

[1] T. Schmugge, P. Gloersen, T. Wilheit, and F. Geiger, "Remote sensing of soil moisture with microwave radiometers," Journal of Geophysical Research (1896-1977), vol. 79, no. 2, pp. 317-323, 1974/01/10 1974, doi: https://doi.org/10.1029/JB079i002p00317.

[2] T. J. Jackson et al., "Validation of Soil Moisture and Ocean Salinity (SMOS) Soil Moisture Over Watershed Networks in the U.S," IEEE Trans. Geosci. Remote Sens., vol. 50, no. 5, pp. 1530-1543, 2012, doi: 10.1109/TGRS.2011.2168533.

[3] M. S. Yee, J. P. Walker, C. Rüdiger, R. M. Parinussa, T. Koike, and Y. H. Kerr, "A comparison of SMOS and AMSR2 soil moisture using representative sites of the OzNet

monitoring network," Remote Sens. Environ., vol. 195, pp. 297-312, 2017/06/15/ 2017, doi: https://doi.org/10.1016/j.rse.2017.04.019.
[4] T. Zhao et al., "Retrievals of soil moisture and vegetation optical depth using a multi-channel collaborative algorithm," Remote Sens. Environ., vol. 257, p. 112321, 2021/05/01/ 2021, doi: https://doi.org/10.1016/j.rse.2021.112321.
[5] Z. Peng et al., "First mapping of polarization-dependent vegetation optical depth and soil moisture from SMAP L-band radiometry," Remote Sens. Environ., vol. 302, p. 113970, 2024/03/01/ 2024, doi: https://doi.org/10.1016/j.rse.2023.113970.
[6] L. Hu et al., "A twenty-year dataset of soil moisture and vegetation optical depth from AMSR-E/2 measurements using the multi-channel collaborative algorithm," Remote Sens. Environ., vol. 292, p. 113595, 2023/07/01/ 2023, doi: https://doi.org/10.1016/j.rse.2023.113595.
[7] K. A. McColl et al., "Global characterization of surface soil moisture drydowns," Geophys. Res. Lett., vol. 44, no. 8, pp. 3682-3690, 2017/04/28 2017, doi: https://doi.org/10.1002/2017GL072819.
[8] P. J. Shellito et al., "SMAP soil moisture drying more rapid than observed in situ following rainfall events," Geophys. Res. Lett., vol. 43, no. 15, pp. 8068-8075, 2016/08/16 2016, doi: https://doi.org/10.1002/2016GL069946.